Polymer Chemistry

Stille Polycondensation: A Multifaceted Approach towards the Synthesis of Polymers with Semiconducting Properties

Journal:	*Polymer Chemistry*
Manuscript ID	PY-REV-07-2023-000815.R1
Article Type:	Review Article
Date Submitted by the Author:	09-Sep-2023
Complete List of Authors:	Liang, Zhen; Zhejiang Sci-Tech University Neshchadin, Andriy; University of Chicago Division of the Physical Sciences Zhang, Zhen; University of Chicago Division of the Physical Sciences Zhao, Fugang; Zhejiang Sci-Tech University, Chemistry and Materials Liu, Xunshan; Zhejiang Sci-Tech University, CHEMISTRY Yu, Luping; University of Chicago, Chem

SCHOLARONE™
Manuscripts

Stille Polycondensation: A Multifaceted Approach towards the Synthesis of Polymers with Semiconducting Properties

Zhen Liang,[a] Andriy Neshchadin,[b] Zhen Zhang,[b] Fu-Gang Zhao, [a] Xunshan Liu,[a,*] Luping Yu[b,*]

[a] Key Laboratory of Surface & Interface Science of Polymer Materials of Zhejiang Province, School of Chemistry and Chemical Engineering, Zhejiang Sci-Tech University, 928 Second Street, Hangzhou, 310018, China

[b] Department of Chemistry and the James Franck Institute, The University of Chicago, 929 E57th Street, Chicago, Illinois, 60637, United States

* Corresponding author: xliu350@zstu.edu.cn; lupingyu@uchicago.edu

ABSTRACT: Recent years have witnessed the rapid development of numerous organic polymer-based semiconductors for applications in areas ranging from organic electronics to bioimaging and biosensing. In the synthesis of these polymer materials, Stille polycondensation has emerged as a highly versatile and effective tool owing to its mild reaction conditions, functional group tolerance, and versatility. This perspective provides a thorough review of the most representative studies post 2011 that highlight the utility of this polymerization method, while also addressing various concerns that researchers may encounter, such as mechanistic insights into Stille polycondensation, potential toxicity, and new polymer structure and functionalities. Furthermore, an alternative approach to the Stille reaction that involves C-H activation is also discussed, providing researchers with additional possibilities for the synthesis of these critical compounds.

1. Introduction

Since the discovery of the Ullmann reaction in 1901, chemists have sought to develop more versatile methods to create carbon-carbon bonds. Of particular importance is the development of techniques for the synthesis of organic semiconductors, which are almost exclusively produced via sp^2-sp^2 cross-coupling reactions such as the Heck, Suzuki-Miyaura, Sonogashira, and Yamamoto reactions. Among these methods, the palladium-catalysed Stille condensation reaction between halides and stannanes shows remarkable tolerance to various functional groups under mild reaction conditions and was used to synthesize a wide range of molecular and polymeric materials with high yields.[1, 2] Studies have demonstrated that Stille polycondensation generates polymers with high molecular weights and narrow polydispersity indices. These polymeric materials have been utilized as functional components in numerous organic optoelectronic devices, such as organic photovoltaic (OPV) solar cells, organic field-effect transistors (OFETs), organic light-emitting diodes (OLEDs), organic light-emitting transistors (OLETs), sensors, and actuators.

Nonetheless, Stille reaction exhibits unique disadvantages, including generations of toxic compounds such as trialkyltin (SnR_3X, X=Cl, Br) and halogenated by-products, which present significant challenges to the principles of green chemistry. This review provides an update on the mechanisms, toxicity issues of tin-containing compounds, and newly synthesized polymeric materials using Stille poly-condensation, with a focus on developments post-2011. This review is not intended to be exhaustive, and readers are encouraged to refer to our previous review.[1]

2. Mechanistic insights

2.1 General mechanism of Stille reactions

The mechanism of the Stille reaction involves three main steps: oxidative addition, transmetallation, and reductive elimination. [2-4] Transmetallation, which is most often the rate-limiting step, can occur through open, cyclic, or ionic transition states (**Figure 1**). The catalyst is a mono- or bidentate Pd(0) complex. For Pd(II) sources, stoichiometric reduction with organostannanes is necessary to generate Pd(0). [1] In cross-coupling reactions for the synthesis of small molecules, the stoichiometric reduction step generally does not pose as much of a problem. However, during polycondensation reactions, the growing chain can compete with the monomers in this step, leading to homocoupling defects.

The Pd(0) complex undergoes oxidative addition of aryl chlorides, bromides, iodides, or triflates, yielding a 16-electron square planar cis-adduct PdL_2ArX. [5] This cis-complex then rapidly isomerizes into the more reactive trans-intermediate due to the trans-effect of ligands. [6] Several subsequent pathways exist for transmetallation, depending on various factors such as reaction conditions, ligands, and solvents. [7, 8]

In the cyclic mechanism, dissociation of the ligand occurs simultaneously with the formation of a bond with an aryl carbon and an interaction between the tin atom and the leaving halogen or triflate. In the open transition state pathway, the halogen on palladium does not interact with tin directly.[2] As for the ionic mechanism, which is facilitated by polar solvents such as toluene-DMF mixtures, involves dissociation of the complex, and the introduction of solvent molecules into the complex inner sphere. This results in a

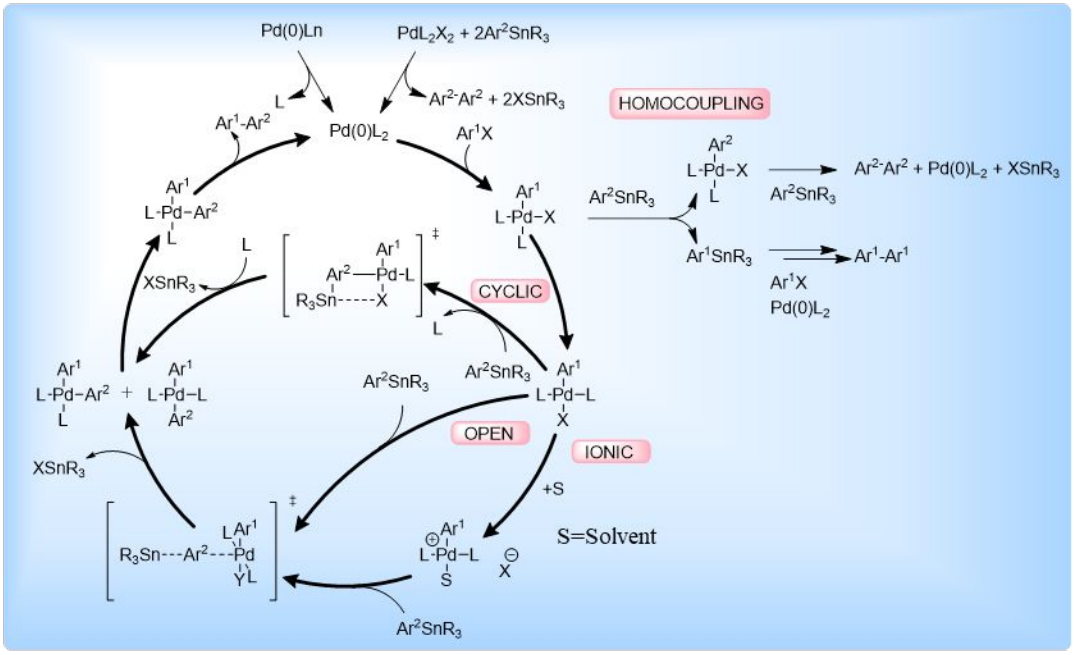

Figure 1. General mechanism of the Stille reaction.

positively charged palladium complex that reacts with the organostannane. All three pathways ultimately lead to a mixture of cis- and trans-diarylpalladium intermediates that must undergo isomerization into cis-complexes. Reductive elimination of biaryl species leads to regeneration of Pd(0), which continues the catalytic cycle.

Homocoupling can occur during Stille polycondensation when, after oxidative addition, PdL_2ArX species instead of undergoing transmetallation undergo aryl-aryl exchange with the organostannane. [9] This exchange results in a different Pd-complex and a new organostannane that can enter the catalytic cycle, creating defects in the polymer chain. The real complexity of the reaction, however, is beyond what discussed here. For example, Palladium can also form π-complexes with monomers, growing polymer chains, intermediates, additives, and solvent molecules, as well as forming poorly characterized palladium black. In these scenarios, heterogeneous or quasi-heterogeneous catalysis need to be considered. [10-12]

2.2 Characteristics of Stille polycondensation

The Stille polycondensation reaction mechanism is very similar to that of the Stille coupling reaction, with the main difference being the reaction substrates involved. [2, 3, 13] As the polymerization process progresses, the size of the reactive substrates increases in a step-wise manner. This, in turn, affects the reactivity of the halide or stanannyl groups and can also impact the reactivity of other functional groups. For instance, the reactivity of the trialkyl stanannyl groups may be altered by the formation of dimers after the first coupling step. However, as the polymerization continues, the reactivity of functional groups should be stablized. Achieving the optimal synthesis of polymers with desirable properties will thus require a thorough exploration of reaction conditions, potential side reactions, and the design of optimal catalytic systems. By understanding the intricacies of the Stille polycondensation reaction mechanism and its impact on polymer properties, researchers can develop more effective strategies for creating polymers with enhanced performance characteristics. As such, studies about reaction conditions, side reactions, and catalytic systems are essential.

3. Stille polycondensation towards functional polymers for various applications

Stille polycondensation is highly advantageous due to its ability to tolerate a wide range of functional groups and yield very high polymerization rates for various monomers. This versatility in accommodating monomers with diverse electronic properties has facilitated the extensive development of organic semiconducting materials, which exhibit intriguing electro-optical characteristics. These materials have been instrumental in the creation of functional components used in a variety of fields, including organic electronics such as organic photovoltaics (OPV), organic field-effect transistors (OFET), organic light-emitting diodes (OLED), and other applications. This segment will delve deeper into the newly developed materials and their relevant properties.

3.1 Polymers applied for solar cells

3.1.1 Background and fundamental principle

Polymer solar cells (PSCs) have emerged as a highly dynamic research field that has experienced significant growth over the past two decades. Despite their lower sunlight-to-electricity conversion efficiency and overall stability when compared with Si-based inorganic solar cells, PSCs possess promising applications in areas such as transparent window coatings, flexible and portable solar panels, and wearable electronics. With the potential for large-scale roll-to-roll production, PSCs are positioned to serve as a low-cost and environmentally-friendly energy source. Successful implementation of PSCs hinges on

optimizing several critical steps, including light absorption, exciton diffusion, exciton separation, and charge carrier transport. Rational structural design and easily accessible synthetic methodologies are necessary to improve each of these processes. In this regard, Pd-catalyzed cross-coupling polycondensation reactions, specifically Stille coupling, have proven highly effective in generating pre-designed conjugated polymers in high yields. [14, 15]

3.1.2 Different OPV polymers generated with Stille polycondensation

Over the past 10 years, research efforts have been largely focused on modifying various organic photovoltaic (OPV) systems. One prominent example is the use of benzo[1,2-b:4,5-b']dithiophene (BDT) as a key building block in donor-acceptor conjugated copolymers. [16] Researchers such as Yang and colleagues have introduced alkyl phenyl and alkylselenyl side groups onto the BDT unit, which were then polymerized with electron-deficient blocks like diketopyrrolopyrrole (DPP) and fluorinated thioeno[3,4-b]-thiophene (TT) via Stille polycondensation using $Pd(PPh_3)_4$ as a catalyst and Toluene/DMF as a solvent system (as shown in **Scheme 1)**. [17, 18] Despite some challenges in achieving reasonable molecular weight (Mn) and a relatively high polydispersity index (PDI) of around 4.4 from PBDTSe-TT, selenium replacement has been found to be critical towards achieving efficient power conversion efficiency (PCE) of 8.8% without the need for any solvent additive or special interfacial layer. These recent findings represent important developments in the field of OPV and pave the way for future research on novel organic materials that can enhance the performance of these devices even further.

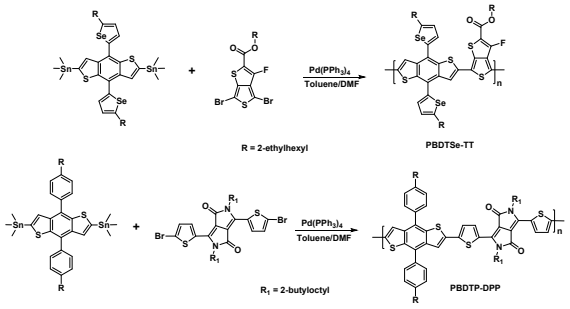

Scheme 1. Synthetic route of **PBDTSe-TT** and **PBDTP-DPP**.

Yu and colleagues undertook a research project that involved exploring a range of polymers that contained fused electron donors (**Scheme 2**). [19-21] Their investigation focused on the correlation between the fused conjugated systems and OPV performance. They synthesized all the donor-acceptor copolymers by utilizing Stille coupling reactions with fluorinated thioeno[3,4-b]-thiophene as the electron donor. The extended conjugation system enhanced molecular planarity, but it also reduced solubility and processability of the polymers. Hence, to achieve a good charge transporting ability and optimal performance in solar cell devices, the authors modified the chemical structures and optimized the device configurations. The authors reported the donor-acceptor energy level match by summarizing all the copolymers they investigated. [21] Out of all the copolymers, polymer PTDBD2, blended with PC71BM, achieved a PCE of 7.6%. When synthesizing these polymers through Stille polycondensation, it is crucial to maintain the solubility of the polymers. However, the fused building blocks decreased the solubility of the resulting polymers. Nonetheless, the authors mitigated this effect by incorporating longer and bulkier alkyl chains, which resulted in product yields up to 94.4% and a high Mn of 46.3 kDa.

Isoindigo building block is an attractive compound in organic electronics because of its excellent optoelectronic properties as well as good structural planarity. McCulloch and team reported an eight-ring fused Thieno[3,2-b][1]benzothiophene isoindigo since they were interested in investigating its copolymerization with thiophene via Stille polycondensation using $Pd_2(dba)_3$ and P(o-tolyl)$_3$ as catalysts (**Scheme 3a**). [22] By controlling the polymerization time and temperature, they were able to synthesize various polymers with molecular weights up to 151 kDa and relatively low PDI levels of 2.7. The resulting polymer, TBTIT, exhibited a large absorption coefficient, high degree of crystallinity, and high charge mobility. Therefore, the device derived from TBTIT:PC71BM yielded an efficiency of up to 9.1% without any additives or thermal annealing process. On the other hand, Bronstein and colleagues described the synthesis of another fused indigoid structure (**Scheme 3b**). [23, 24] They generated a series of good performance polymers by copolymerization with different monomers via Stille coupling reaction, with one example being polymer INDT-T, which displayed an extremely low bandgap with maximum absorption at around 800 nm. This copolymer exhibited remarkable ambipolar charge transfer properties, with hole-to-electron mobility of 0.23 $cm^2\ V^{-1}\ s^{-1}$/0.48 $cm^2\ V^{-1}\ s^{-1}$ due to its large conjugated system and high molecular crystallinity.

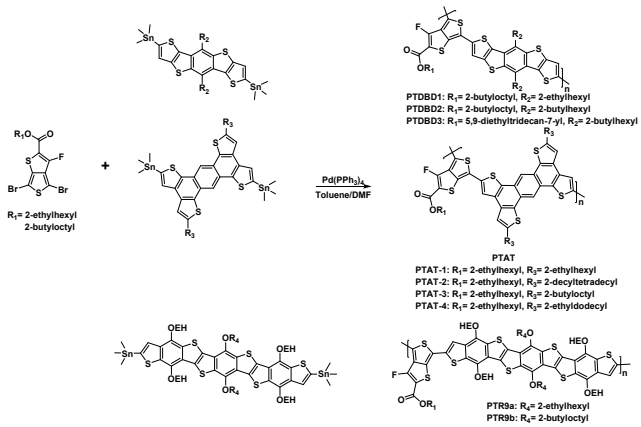

Scheme 2. Synthesis of donor-acceptor copolymers with electron-rich units possessing extended conjugation.

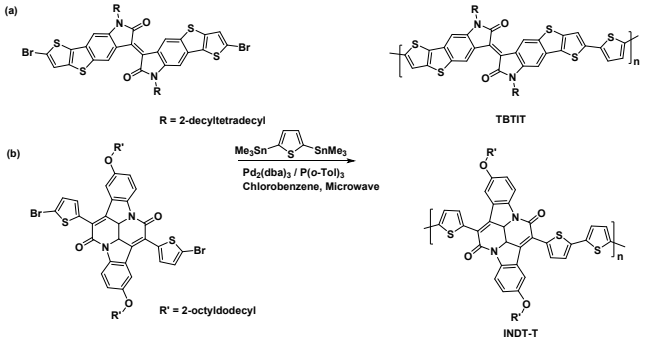

Scheme 3. Synthetic route to Isoindigo-containing polymers.

Instead of solely focusing on modifying the structure of BDT units, Yu and colleagues took a different approach by synthesizing a range of electron-deficient units and subsequently copolymerizing them with the BDT units through Pd-catalyzed Stille coupling reactions, as demonstrated in **Scheme 4**. [9, 25-27] As a means of ensuring effective solubility of the reaction mixtures and generating high Mn for the resulting polymers, chlorobenzene was utilized as a solvent for the synthesis of PID and PPB. Following the synthesis, the researchers systematically evaluated the impact of internal dipole moments and polymer dispersity ($Đ$) on solar cell performance. Their findings revealed that the local dipole moment in the polymer backbone allowed for enhanced charge transfer from the polymer to PCBM, ultimately leading to improved device performance.

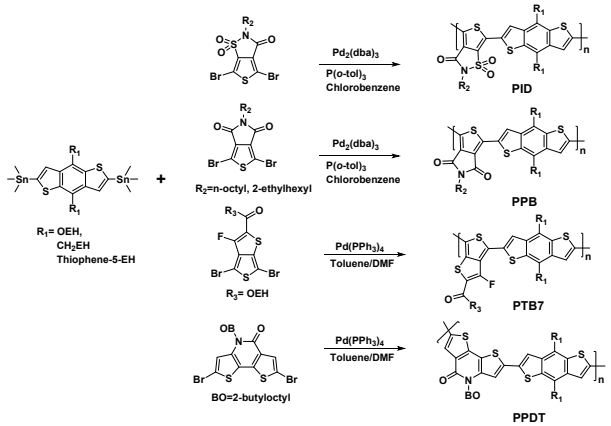

Scheme 4. Synthesis of BDT-containing copolymers with various electron-deficient units.

Yang et al. synthesized a series of PBDTT-DPP derivatives with similar Mn of approximately 38 kDa and a low PDI of 2.1 using Stille coupling reactions (**Scheme 5**). [28] Notably, attempts to increase the molecular weight beyond 38 kDa resulted in poor solubility and hindered solution-processing. Subsequently, the effect of various heteroaromatic bridges, namely furan, thiophene, and selenophene, was investigated systematically. The replacement of either the oxygen or sulfur atoms in the DPP unit with selenium led to a lower bandgap and an increase in hole mobility, as well as a significant improvement in the performance of the material. Of this series, PBDTT-SeDPP exhibited a photo-current of 16.8 mA/cm^2 and a PCE of 7.2% in a single junction PSC device, outperforming its PBDTT-FDPP or PBDTT-DPP counterparts. These findings offer important insight into the design and optimization of high-performance conjugated polymers for use in optoelectronic devices.

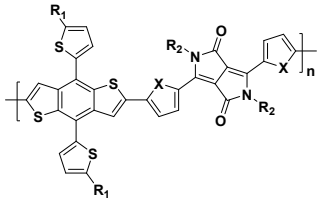

Scheme 5. Chemical structures of PBDTT-DPP derivatives

In 2014, McCulloch and his team carried out a systematic investigation into the influence of chalcogenophene comonomers, including thiophene, selenophene, and tellurophene, on the properties of DPP-TT copolymers. These copolymers were synthesized using Stille coupling reactions under microwave assistance (as demonstrated in **Scheme 6**) [29] and were then subjected to Soxhlet extraction for purification. The chloroform portion was also treated with diethyldithiocarbamic acid diethylammonium salt in order to eliminate any residual palladium compound. It was discovered that the introduction of heteroatoms gradually reduced the bandgap of the polymers by stabilizing the LUMO energy levels. Larger heteroatoms further improved intermolecular heteroatom-heteroatom interactions, ultimately resulting in an improvement in hole mobility. These heteroatom-containing polymers exhibited promising photovoltaic properties, with power conversion efficiency (PCE) ranging from 7.1% to 8.8% in an inverted device configuration. It is important to note that the replacement of sulfur atoms with either selenium or tellurium does not always lead to an improvement in device performance, which is usually dependent on a trade-off between V_{OC}, charge carrier mobility, and film morphology.

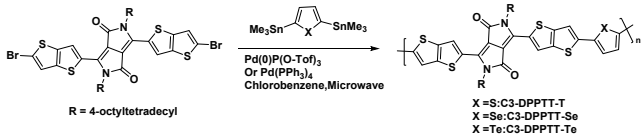

Scheme 6. Synthetic route to chalcogen-containing DPP-TT copolymers.

Heeney and his team utilized the Stille polycondensation method to synthesize germanium-containing copolymers for use in organic solar cells as shown in **Scheme 7**. [30, 31] The crude polymers were then end-capped to mitigate the potential adverse effects of the terminal bromide. Interestingly, longer side chains resulted in higher Mn levels compared to shorter chain analogs due to improved solubility, despite performing the Stille reaction in chlorobenzene with the assistance of microwave radiation. The physical and optoelectronic properties of the polymers were thoroughly examined, taking into account different electron-deficient groups, as well as varying lengths and alkyl side chains. The resulting solar cell devices based on

pDTTG-TPD and $PC_{71}BM$ demonstrated a significantly impressive efficiency of up to 7.2%, without any need for thermal annealing or processing additives. In 2017, He and his colleagues designed and synthesized a range of chlorinated donor-acceptor type polymers through Stille reactions, utilizing BDT and chlorinated units. [32-35] These new chlorinated polymers exhibited deep HOMO energy levels (approximately 5.5 eV), resulting in increased open-circuit voltage and PCEs as high as 9.11% for a 250-nm-thick active layer. This chlorination technique was initially pioneered by Hou and coworkers when creating chlorinated polymer donors via Stille polycondensation, leading to high PCEs up to 14% for solar cell devices based on these specific polymers. [36]

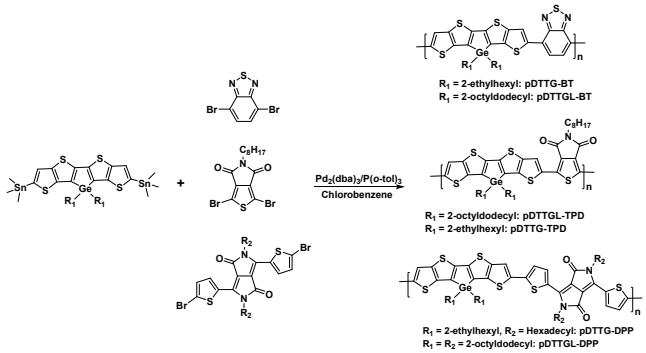

Scheme 7. Synthetic route of germanium-containing conjugated polymers.

Bazan and coworkers synthesized a series of PT-CPDT-PT-containing (PT = pyridyl[2,1,3]thiadiazole, CPDT cyclopentadithiophene) polymers as depicted in **Scheme 8**.[37, 38] Impressively, synthesis of **PIPCP** was carried out at high temperatures up to 200 °C to achieve a good yield of about 81%, indicating the feasibility of Stille polycondensation under harsh reaction conditions. These polymers exhibited low bandgaps in the range of 1.4 - 1.5 eV. It was found that regioregularity, PT orientation (pyridyl N-atoms point toward or away from the CPDT fragment) and the choice of comonomer play important roles in film morphology and device performance. After molecular structure and device optimization, a PCE of around 7.2% was achieved with a V_{oc} loss of 0.6 eV and an EQE of over 60% from the polymer **PM2** (**Scheme 8**) with strictly organized PT orientations. To further understand the origin of the high V_{oc} (0.86 eV) as well as the low energy loss from this system, a more precise energetic landscape for the exciton to charge carrier conversion process is needed.

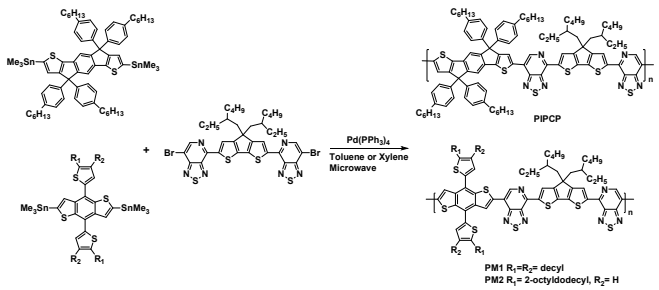

Scheme 8. Synthetic route to PT-CPDT-PT-containing copolymers.

While the majority of copolymers have traditionally been utilized as electron donors in solar cell devices, in 2014, Yu and co-workers paved the way by utilizing Stille polycondensation reaction to synthesize novel electron-accepting polymers. [39] This groundbreaking achievement produced a series of polymers composed of different monomer combinations, allowing for the study of their properties and impact on the relative electron affinity of the monomers. Surprisingly, it was found that the LUMO energy levels of polymers were influenced by the stronger electron-accepting monomers, while the HOMO energy levels were determined by weakly electron-accepting monomers. Jenekhe et al. further advanced this development by copolymerizing naphthalene diimide (NDI) with thiophene and selenophene through the Stille coupling reaction as shown in **Scheme 9 (PNNIT** and **PNNIS-HD)**. By achieving a high molecular weight above 20 kDa with a relatively low PDI of approximately 1.2, they were able to fabricate a complete polymer solar cell device using NDI-selenophene polymer PNNIS-HD and thiazolothiazole copolymer PSEHTT as the donor material, achieving an impressive PCE of 3.3%.[40] Further improvements were achieved by incorporating electron-accepting material PNNIS-HD and PBDTT-FTTE into the electron donor backbone, improving the PCE to 7.7% through a simple film aging process at room temperature. [41] More recently, Li and co-workers successfully developed an all-polymer solar cell by designing a π-conjugated polymer acceptor named **PZ1** through Still polymerization. The acceptor, composed of n-OS IDIC-C16 as the crucial building unit and utilizing thiophene as the π-bridges, exhibited promising performance in solar cell devices. Notably, this innovative polymer acceptor achieved an outstanding power conversion efficiency (PCE) of 9.19%, setting a new record for all-polymer solar cells.[42] Their group further developed the novel rhodamine-incorporated polynaphthalenediimide acceptor **PNDI-2T-TR** as illustrated in **Scheme 9**. [43] Compared with its NDI analog, this new copolymer displayed stronger light absorption, an up-shifted LUMO energy level, and reduced crystallinity, resulting in an impressive PCE of 8.13% when paired as a donor material with **PBDB-T** (**Scheme 9**). These all-polymer solar cells showed even further improvements when electron-withdrawing blocks, commonly used as small molecule acceptors for solar cell devices, were introduced into the electron-accepting polymer backbones.

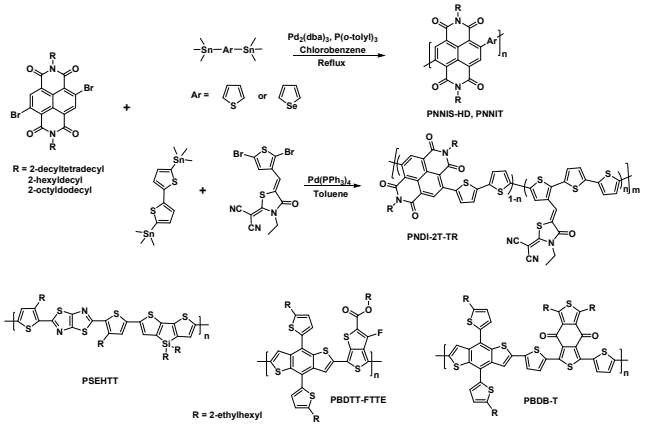

Scheme 9. Synthetic route of NDI-containing copolymers and **PNDI-2T-TR**.

Yan and colleagues employed microwave radiation to enhance the reaction rate and improve yield (76%), during the synthesis of a copolymer called PFBDT-IDTIC as shown in **Scheme 10**.[44] The copolymer was composed of alternate BDT and IDTIC moieties, which were linked through Stille polycondensation, as presented in **Scheme 10.** The resulting polymer showcased good solubility in commonly used organic solvents such as chloroform, chlorobenzene, and toluene. In addition, it exhibited excellent electron mobility and large absorption coefficient. When blended with electron donor material **PM6** (**Scheme 10**), the all-polymer solar cells demonstrated a remarkable power conversion efficiency (PCE) of 10.3% after optimization. These findings highlight the successful development of a high-performing, all-polymer solar cell device.

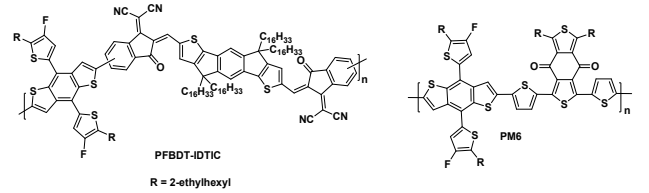

Scheme 10. Chemical structures of **PFBDT-IDTIC** and **PM6**.

Over the past five years, there has been extensive research into non-fullerene solar cells and even all-polymer solar cells.[45, 46] The emergence of non-fullerene acceptors, which offer synthetic versatility, strong absorption abilities and high thermal stability, has led to impressive power conversion efficiencies of more than 18% in single junction devices. Polymeric acceptors have been widely adopted and have shown excellent performance. Novel polymer donors such as PM6 and D18, which were developed using Still polycondensation, have also demonstrated impressive device performances.[47-49] In particular, some easily synthesized and cost-effective polymer donors based on TzCl, such as PTz3Cl and PBTTz3Cl, have been developed through Still polycondensation, without alky chain substituted thiophene π bridges.[50] These polymers exhibited exceptional power conversion efficiencies exceeding 19%. Additionally, the polymer PBTTz3Cl showcased excellent applicability in fabricating high-performance PSCs using a variety of narrow-bandgap small molecular acceptor materials, including IT-4F, Y6, N3, BTP-eC9, and L8-BO. Significantly, a few polythiophenes materials synthesized through Still reactions have been utilized for blending with small molecular acceptors in solar cell devices. These materials have demonstrated exceptional performance by precisely tuning the energy levels of the polymer materials.[51, 52] Achieving consistent batch-to-batch reproducibility and simplifying the synthesis process pose significant challenges for scaling up solar polymers production. In order to address these challenges, Cao et al. have proposed a novel approach to synthesizing a donor polymer using 3-cyanothiophene as a base via Still polycondensation. Through control of regioregularity, they have successfully demonstrated superior batch-to-batch reproducibility and commendable performance. This innovative method holds great promise in facilitating the development of large-scale production and ensuring the stability of polymer performance. This approach signifies a commendable strategy for the advancement of mass production and the attainment of performance durability in solar cell polymers.[53] Consequently, the Stille reaction continues to be an indispensable method for synthesizing new sets of polymer materials. This underscores its significance in the field of polymer synthesis.[54-60]

3.2 Copolymers for Organic field-effect transistors (OFET)

Organic field-effect transistors (OFETs) possess several distinct advantages, including low-cost, large surface area, and flexibility. To achieve optimal performance, OFET materials should showcase high carrier mobility, a large Ion/off ratio, a small threshold voltage, and energy levels that align with the work function of electrodes. Hence, the ideal material should exhibit a tunable structure that enables the desired properties to manifest. Donor-Acceptor conjugated copolymers have been identified as a promising choice for OFET materials. Over the past decade, many new monomeric moieties have been synthesized, providing an expanded library of building blocks for copolymerization. To effectively assemble the monomeric units, the Stille polycondensation method has been extensively utilized, yielding high-performance polymers with easily functionalized monomers.[61-72] These advances have led to the development and application of several high-performance polymers in OFET technology.

Numerous conjugated polymer systems containing DPP moieties have demonstrated high carrier mobilities and exceptional device performance. In 2013, Jo and colleagues investigated the impact of fluorine substitution on energy levels, crystal orientation, and charge-carrier transport in a series of DPP-based conjugated copolymers. [73] The researchers discovered that the addition of fluorine significantly improved planarity, altered LUMO energy levels, and changed charge transport behavior within the transistor. Of particular note, the polymer **DPPPhF4** (**Scheme 11**), which contained four fluorine substitutions, exhibited outstanding n-type charge-transport behavior with an impressive electron mobility of 2.36 $cm^2 V^{-1} s^{-1}$. Furthermore, OFET devices containing this polymer showed excellent air stability and consistent performance over a 7-month ambient storage period. It is worth highlighting that the synthesis of DPPPhF4 required only a

three-hour microwave reaction in a Toluene/DMF mixture, significantly reducing the reaction time while still producing reasonable molecular weights (16.3 kDa), polydispersity (1.79), and yields (63%) compared to a typical Stille polycondensation.

Kwon et al. successfully synthesized a D-A copolymer named PDPPDTSE with high yields (94%) and a relatively high molecular weight (61.9 kDa), employing Stille reaction to couple DPP and selenophenylene vinylene selenophene monomers. [74] The polymerization process took 48 hours. Astonishingly, the polymer exhibited an ordered structure after annealing, which resulted in a remarkable carrier mobility of 4.97 $cm^2\ V^{-1}\ s^{-1}$ (Ion / Ioff = 1.55×10^7) when applied to OFET devices. The vinyl linked selenophene vinylene selenophene unit in PDPPDTSE (**Scheme 11**) extended the conjugation length, paving the way to enhanced intermolecular interactions. Furthermore, the relatively mobile lone pair of selenophene atoms played a vital role in boosting the chain interactions between the neighboring chains, enhancing the overall performance of the polymer.

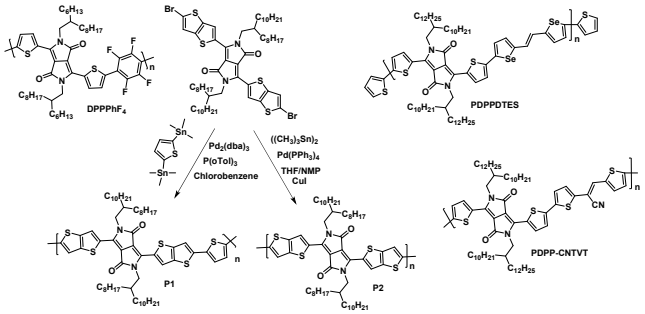

Scheme 11. Structures of some DPP-based semiconductor polymers.

In 2014, a groundbreaking electron mobility record, 7.0 $cm^2\ V^{-1}\ s^{-1}$ in OFETs was achieved by Kwon and coworkers with the development of the DPP-based D-A polymer PDPP-CNTVT (**Scheme 11**). [75] Utilizing Stille polycondensation, the polymer was able to achieve an exceptionally high molecular weight of 125.2 KDa. To enhance the efficiency of the polymer, the authors incorporated a nitrile group onto the rigid vinylene linkage, resulting in an electron-deficient backbone and transforming the polymer into an n-channel material. Furthermore, careful consideration was given to the optimal incorporation point of the nitrile group to avoid steric effects while preserving the coplanarity of the polymer and maintaining a high carrier mobility.

In 2017, Liu and colleagues reported a series of copolymers with an A1-D-A2-D configuration based on naphthalenediimide-benzothiadiazole that had heteroatom substitutions. [76] These copolymers were synthesized using Stille polycondensation. The authors investigated the effects of heteroatom substitution on polymer performance and discovered that selenium atoms have a larger p-orbital compared to sulfur atoms in thiophene heterocycles. This resulted in stronger interactions between polymer chains, leading to improved crystallization, organization, and interchain charge carrier transport. Among the four polymers tested, polymer **PNBS** (**Scheme 12**) exhibited the best performance in an air-stable OFET with an exceptional electron mobility of 8.5 $cm^2\ V^{-1}\ s^{-1}$. This study enriches our understanding of heteroatom substitutions on polymer properties and provides potential opportunities for enhanced performance in electronic applications.

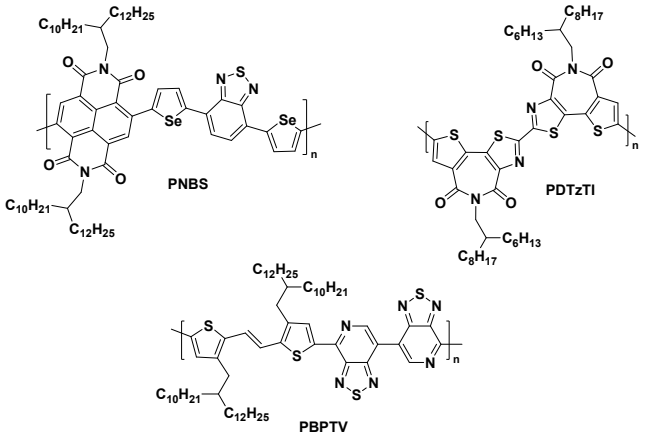

Scheme 12. Structures of some good performance polymers for OFETs.

In the same year, Liu and co-authors made a breakthrough by synthesizing a highly efficient ambipolar semiconducting polymer **PBPTV** (**Scheme 12**) utilizing regioregular bis-pyridal[2,1,3]-thiadiazole (BPT) acceptor. [77] The unique molecular structure of PBPTV exhibited strong electron-withdrawing capacity, resulting in a low LUMO energy level and strong electron affinity for the copolymer. In particular, the addition of the BPT unit led to a relatively high hole mobility of 6.87 $cm^2\ V^{-1}\ s^{-1}$ and electron mobility of 8.49 $cm^2\ V^{-1}\ s^{-1}$. Notably, PBPTV was synthesized using (E)-1,2-bis(tributylstannyl)ethene as a monomer, and the catalytic system and reaction conditions were optimized. There was no explicit explanation given for the choice of the new method, but it could be attributed to the difficulty in obtaining a pure ditin TVT monomer, which had long branched chains that made it challenging to crystallize. This study highlighted the versatility and flexibility of Stille reactions, making it a promising tool for the synthesis of novel polymer materials.

In 2018, Guo and colleagues synthesized a novel all-acceptor homopolymer **PDTzTI** with an imide-functionalized thiazole backbone (**Scheme 12**). This synthesis was particularly interesting because the researchers had to overcome several challenges to obtain a symmetric dibromo-monomer. They achieved this by carrying out a homo-polymerization reaction using only one monomer, in contrast to normal Stille polymerization methods that require multiple monomers. [78] This novel approach broadens the use of electron-deficient building blocks for all-acceptor polymers. Physicochemical studies revealed that the resulting polymer, PDTzTI, exhibited unipolar electron transport behavior with a relatively high electron mobility of 1.61 $cm^2\ V^{-1}\ s^{-1}$ in an OFET device. The polymer also demonstrated a remarkably high current on/off ratios of 10^7–10^8, showcasing its potential for use in high-performance electronic devices. The relatively planar structure of the polymer backbone facilitated intermolecular charge mobility and enhanced the material's crystallinity, critical factors for carrier mobility. Overall, the research findings demonstrate the potential of the Stille polymerization method for synthesizing electron-deficient

building block-based polymers with desirable electronic properties, such as unipolar electron transport. The unique synthesis method employed by Guo and colleagues represents a significant advancement in polymer chemistry, with widespread applications in the development of high-performance electronic devices.

3.3 Synthesis of other functional polymers

In recent years, the versatility of Stille polycondensation is also manifested in the development of other functional polymers for applications in photocatalysts, bioimaging materials, and optical and magnetic materials. Several examples shown below illustrate the utility of this polymerization method.[63, 79-89]

Yu and colleagues successfully synthesized a novel conjugated D-A copolymer known as PBDT-bpy through the use of Stille polycondensation. [90] This polymer proved to be an effective polymeric ligand that can coordinate with cobalt ions to form a complex polymer, which was thoroughly investigated as a heterogeneous photocatalyst for hydrogen evolution. The results demonstrated that the PBDT-bpy polymer exhibits remarkable catalytic activity for hydrogen evolution when triethanol amine is utilized as a sacrificial agent. This research clearly indicates that metal-chelating conjugated polymers offer a wealth of opportunities for the rational molecular design of photocatalysts for hydrogen evolution from water.

Patra and team employed Stille polycondensation to synthesize two homopolymers based on Benzodithieno-imidazole (**Scheme 13**). [91] Interestingly, they were successful in directly polymerizing the freshly prepared ditin-monomer 6 with the dibromo monomer 5 under mild reaction conditions in THF at 65 ^{o}C. The resulting polymers exhibited narrow polydispersity indexes and reasonable molecular weights (around 15 kDa). Optical studies revealed that the conjugated polymer P2 serves as an excellent fluorescence sensor for detecting paramagnetic Cu^{2+} ions, displaying high sensitivity and selectivity through fluorescence quenching via photoinduced electron transfer. The fluorescence intensity of **P2** decreased linearly with the concentration of Cu^{2+}, indicating that it has great potential as a selective probe for detecting Cu^{2+} ions in the presence of other metal ions. This research presents a novel paradigm for further development of soluble π-conjugated fluorescent polymer-based probes by fine-tuning the electronic factors that enable them to sense environmentally relevant metal ions.

Wang and colleagues utilized Stille polycondensation to develop a highly efficient D-A copolymer (**TBDOPV-DT**, **Scheme 13**) with a narrow optical band gap (0.98 eV) and strong near-IR absorption. [92] The researchers investigated the photothermal energy conversion capabilities of this polymer and discovered that immediate exciton returns to the ground state via IC contributed to efficient conversion. Additionally, this conjugated polymer displayed exceptional stability, making it highly suitable for repeated use. This work's chemical approach can be widely applied to fabricate more near-IR absorbing polymer materials that can function as photodetectors and photo filters.

Swager and colleagues report on the synthesis of a series of stable radical polymers based on 1,3-bisdiphenylene-2-phenylallyl (**RP, Scheme 13**) using Stille polycondensation. [93] Post-deprotection and oxidation were also employed in their fabrication. These radical polymers are ambipolar conductivity materials that also exhibit redox activity. Interestingly, the polymers present magneto-optic (MO) properties with Faraday rotations, with the sign of optical rotation being modulated by the radical character. The absolute Verdet constants of up to 2.80 ± 0.84 ×10^4 deg T^{-1} m^{-1} at 532 nm were recorded. All of these materials were successfully synthesized via Stille reaction. Moreover, many other organic semiconductor copolymers have been developed using Stille polycondensation, such as wearable electronics, self-healing materials, [94, 95] biological imagers, gas sensors, and in vivo photoacoustic imagers. [96] Promisingly, modifying reaction conditions and designing new monomers could yield a vast catalogue of valuable polymers with widespread applications.

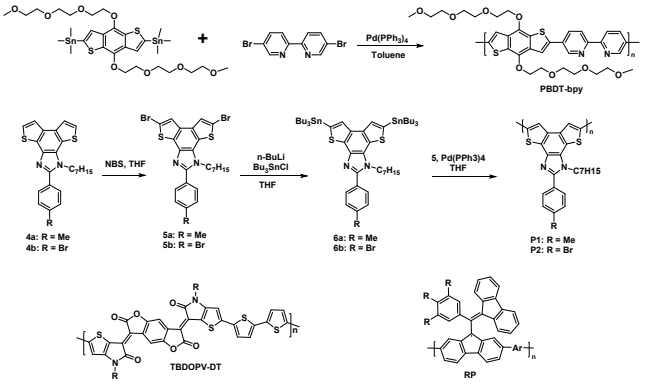

Scheme 13. Synthetic routes and structures of some example polymers for applications other than organic electronics.

4. Potential issues in the Stille polycondensations

The main drawback of Stille polymerization is the occurrence of homo-coupling reactions between ditin or dibromo monomers, leading to structural defects in the polymer chain, decreased molecular weight, and increased polydispersity indexes, consequently impacting the properties of the resulting polymers. In 2014, Janssen and colleagues investigated the effect of intrachain homocoupling defects on alternating push-pull semiconducting PDPPTPT polymers based on dithienyl-diketopyrrolopyrrole and phenylene using Stille polycondensation as a model. They examined the optical properties and performance of the polymers as donor materials in OPV solar cells and found that those with homocoupling defects exhibited red-shifted shoulders in their UV-vis spectra and decreased performance in optoelectronic devices, such as lower PCE in OPV solar cells. [97] It has been observed that the structure of the monomer has an impact on the occurrence of homocoupling defects in the synthesized polymers. Maes and co-workers synthesized a series of polymers by copolymerizing dibromo quinoxaline and dibromo biquinoxaline via Stille polycondensation to quantify and control the number of homocoupling defects. Their results showed that the homocoupled acceptor dimer caused a blue-shift in the absorption peaks due to polymer chain twisting, leading to reduced photocurrent and fill-factor. [98]

Polydispersity indexes (PDI) are closely tied to the properties of polymers, and can significantly impact their performance. A study by Yu et al. investigated the effects of PDI on the performance of polymer-based solar cells, examining a range of polymers with varying PDIs. [9] The study found that larger PDIs were associated with structural defects that acted as energy transfer and charge trapping/recombination centers, ultimately leading to a reduction in power conversion efficiency. Specifically, in devices based on the polymer PTB7, the efficiency fell from 7.59% to 2.55% as the PDI increased from 2.1 to 4.3, due to reduced short-circuit current, open-circuit voltage, and fill factor. The study emphasized the importance of reaction time in controlling PDI.

The selection of a suitable catalyst is of utmost importance in regulating defects during the synthesis of conjugated polymers. In a study conducted by Chochos and colleagues, they found that the use of $Pd_2(dba)_3$ in a 1:2 ratio with the sterically hindered o-Tol3P resulted in conjugated polymers with higher molecular weights, narrower polydispersity distribution, lower percentages of homo coupled defects, and higher absorbance coefficients than those synthesized using $Pd_2(dba)_3/Ph_3P$ or $Pd(PPh_3)_4$. [99] Similarly, in another study conducted by Xu et al., two different catalytic systems, $Pd(PPh_3)_4$ and $PdCl_2(PPh_3)_2$, were used in the synthesis of conjugated polymers based on diketopyrrolopyrrole- (DPP) and thienothiophene. [100] The study revealed that the polymer prepared using $Pd(PPh_3)_4$ as a catalyst demonstrated better electrochromic properties, including a larger optical contrast and coloration efficiency by 40% and 79% respectively, and a faster coloration time by 55% at 825 nm, than the one prepared using $PdCl_2(PPh_3)_2$. Furthermore, $Pd(PPh_3)_4$ resulted in polymers with fewer structural defects. Overall, these studies demonstrate the critical role played by the choice of catalyst in controlling the quality and properties of conjugated polymers.

Various heating sources have been utilized to aid in the implementation of Stille polymerizations. Researchers led by Park discovered that employing microwave-assisted polymerization in the production of M-PTB7(32 k) resulted in a lower photovoltaic conversion efficiency (PCE) of 6.1% compared to that of TPTB7(31k) which yielded a higher PCE of 7.8%.[101] The larger molecular weight of M-PTB7(75k) synthesized under microwave-assisted conditions had a significant negative impact on device performance, yielding a PCE of only 2.8% due to the presence of homo-coupled by-products.

Furthermore, there is also the potential for chain defects in the polymer to arise from the presence of tin and/or halogen end groups, which may act as charge trapping centers. [102-104] To address this issue, Carter and colleagues conducted a study evaluating the end-capping effectiveness of several reagents in the Stille polycondensation of 2,7-dibromo-9,9-bis(2-ethylhexyl)fluorene and 2,5-bis(trimethylstannyl)-thieno[3,2-b]thiophene. [105] Their findings indicate that iodo-compounds exhibit superior end-capping efficiency compared to bromo derivatives.

Manipulation of reaction protocols has also been demonstrated to have a significant impact on the properties of polymers. For instance, Yang and colleagues proposed a stepwise-heating protocol for Stille polycondensation in the PTB7 system. [106] Conventional PTB7 synthesis involves heating the reaction mixture at 120°C for 12 hours, whereas the newly proposed protocol involves heating the reaction mixture initially at 120°C for 1 hour, followed by 60°C for 11 hours, and then 120°C for 1 day. The polymer obtained via the stepwise heating protocol had a significantly higher molecular weight (223 kDa) and a lower polydispersity index (1.21) compared to the traditional PTB7 synthesis method (M_w=75.8 kDa, PDI=1.62). Surprisingly, despite the comparable optoelectronic properties between the two polymers, the PCEs of the new polymer were notably higher, reaching up to 9.97% when blended with PCBM, in contrast to only 8.02% for commercial PTB7 and 6.98% for the conventional polymerization method. In addition, the 30 devices prepared with the newly synthesized polymer exhibited good reproducibility, with only a 5.88% error range. These findings highlight the importance of optimizing reaction conditions for polymer synthesis, as even minor adjustments can significantly impact the performance of resulting polymers. Ultimately, this provides valuable insights into the design of high-performance organic polymeric materials for various optoelectronic applications.

Encouragingly, recent research findings reported by Huang et al. have presented some remarkable strategies for addressing these challenges. They successfully devised a robust and efficient Stille-type cross-coupling polycondensation technique at room temperature, utilizing a Buchwald precatalytic system. The resultant copolymers exhibited exceptional molecular weight and yields, highlighting the success of this methodology. Importantly, the copolymers synthesized using this method demonstrated an absence of homocoupling structural defects.[107] Additionally, Huang and colleagues developed a versatile room temperature aryl disulfide C-S polycondensation methodology, which proved highly effective in facilitating the cross-coupling polymerization between various aryl distannanes and aryl bis-thioethers. This approach enabled the production of defect-minimized, high molecular weight alternating semiconducting conjugated copolymers.[108] These research findings offer a robust and competitive means of synthesizing polymers, thereby significantly reducing the occurrence of structural defects in high-performance polymer semiconductors.

5. Toxicity of tin byproducts

Trialkylstananne compounds, commonly used as monomers in Stille polycondensation, have been linked to toxic effects on the endocrine system in mammals leading to reproductive complications. [109] Furthermore, research has shown that different organs and systems are adversely affected by these organotin compounds - trimethyl and triethyltin chlorides have been found to predominantly impact the nervous system, while tributyltin targets the immune system. [110] Recent studies have also shown that diorganotin chlorides exhibit neurotoxicity in rat PC12 cells, with dibutyltin chloride demonstrating greater toxicity than diphenyltin chloride and dimethyltin derivative. Apoptosis is induced through a mitochondrial-

mediated pathway with a significant increase in intracellular reactive-oxygen species. These findings highlight the potential hazardous consequences of using these organotin compounds and the need for further research into safer alternatives. [111]

The issue of toxicity associated with tin-containing monomers has been a major drawback of the Stille reaction, prompting the exploration of alternative methods. Nonetheless, there are strategies to mitigate the toxicity or eliminate toxic compounds from the final polymer product. One such approach is to use longer alkyl chains, which have been shown to reduce toxicity significantly. [112, 113] For example, trioctyltin chloride is considered virtually nontoxic, while tributyltin chloride is less toxic than its triethyl and trimethyl counterparts, owing to changes in biological processes as alkyl chains become longer.

However, for Stille polycondensations, highly reactive monomers are required, and these typically demand the use of toxic and high-reactivity tin-containing monomers. Consequently, additional measures are necessary to address the toxicity issue of these monomers. During polymerization, trialkylstannane species may be left attached to the polymer chains, and trialkyl tin end groups can also pose a toxicity concern. To mitigate these issues, several effective methods have been developed, including conversion of trialkyl tin end groups to bromides or iodides, precipitation of tin-containing by-products in methanol, and filtration through celite followed by disposal of the residual waste materials as toxic waste. Organotin compounds can also be readily converted into insoluble polymeric fluorides through filtration with a potassium fluoride-celite mixture. [114]

Further alternative methods include treatment with DBU and water, [115] oxidation and formation of SnS_2, [116] and other modifications, [117, 118] which not only reduce the toxicity of chemical waste but can also be used in high-scale operations at relatively low cost. Despite the challenges associated with toxicity of tin compounds, the Stille polycondensation remains a frequently employed method owing to the availability of effective ways to address the toxicity issues.

6. Alternatives to Stille polycondensation

Aside from the widely used Stille polycondensation, there are numerous other reactions that have been developed for synthesizing semiconducting polymers. [119] Some of these include nickel and palladium-catalyzed cross-couplings like the Heck, Yamamoto, Kumada, Sonogashira, and Suzuki-Miyaura reactions. Regarding the benefits of Still polycondensations, we kindly direct readers to our previously published review article in 2011 for a more comprehensive analysis (Chem. Rev. 2011, 111, 1493-528). With the rapid advancements in the field of organic electronics, newer strategies have emerged for synthesizing polymer materials for a range of applications. One such strategy that has emerged as a powerful alternative to Stille polycondensation is the direct arylation polymerization approach (DARP). [120-124] Through this methodology, unmodified C-H bonds in monomers react with dibromo- or diiodo- compounds to produce conjugated copolymers. An increasing number of studies have compared the optical and electronic properties of polymers made using the DARP method versus those made using the Stille reaction, and have shown that similar properties can be achieved. [122, 125-130] In this article, we will delve into a comprehensive comparison between the Stille reaction and the DARP method.

The DARP method offers a clear advantage over the Stille reaction by avoiding the use of toxic organotin compounds. This has been identified as the main issue of the Stille reaction, as it poses significant health and environmental risks. The DARP method utilizes C-H bonds instead of tin compounds, making it a promising and environmentally-friendly approach. Nevertheless, despite the advantage of simpler starting materials, the DARP method has some limitations. For instance, it tends to generate lower molecular weight polymers compared to those synthesized via Stille polymerization. This can significantly impact the performance and properties of these materials. To address this challenge, Livi et al. extensively optimized DARP conditions for the synthesis of PPDTBT. [125] However, the molecular weights achieved did not exceed 16 kDa, significantly lower than those achieved via Stille polymerization. While the best performing DARP material had similar properties to its Stille alternative of similar molecular weight, another batch of Stille polymer had a molecular weight of 59 kDa and higher power conversion efficiency (PCE) of 3.8%. This work highlights that Stille polymerization has an advantage over DARP methodology due to its greater access to higher molecular weight polymers.

Kruger and his colleagues conducted a study on BDT-TQT polymers with differing side groups, and their research indicated that the PCE of DARP prepared materials can achieve a maximum of 4.4% and 5.8%, while the Stille synthesized versions reached up to 5.6% and 7.3%.[129] The main reason for such a significant difference is the difference in molecular weight, with DARP polymers having Mn=13.7 and 18.2 kDa and Stille polymers having Mn=38.0 and 22.3 kDa. Farinola et al. also conducted a comparison of the DARP and Stille methodologies for the synthesis of ternary random copolymers of BDT and BTD-BTA. [130] The research results showed that the PCE of the polymer prepared via the Stille route was consistently higher than that of the DARP prepared polymers, reaching 2.5% and 4.8% versus 2.1% and 2.8%.[131] These findings highlight the importance of carefully considering the molecular weight of polymers when attempting to maximize PCE.

Matsidic et al. successfully synthesized polymer PNDIT2 using both DARP and Stille routes, with the latter producing polymers boasting hole mobilities of up to 3.2 $cm^2 V^{-1} s^{-1}$. While the DARP method yielded defect-free polymers, the process required extensive optimization. DARP protocols typically employed either the Ozawa method, which necessitated the use of a pressurized vessel and Pd(0) sources such as $Pd_2(dba)_3$ and Cs_2CO_3 in THF or toluene at 110-120°C, or the more popular Fagnou conditions, which utilized $Pd(OAc)_2$ in DMA at 70-110°C and required the additional use of pivalic acid. Tobin Marks group's research revealed that the inclusion of 2,2-diethylhexanoic acid as an additive was essential in producing PNDIT2 materials with superior OPV performances. [132] While carbonates or

carboxylic acids are necessary for proton transfer during Pd-catalyzed couplings, employing sterically hindered carboxylic acids reduces the incidence of branching defects in the final polymer chain.

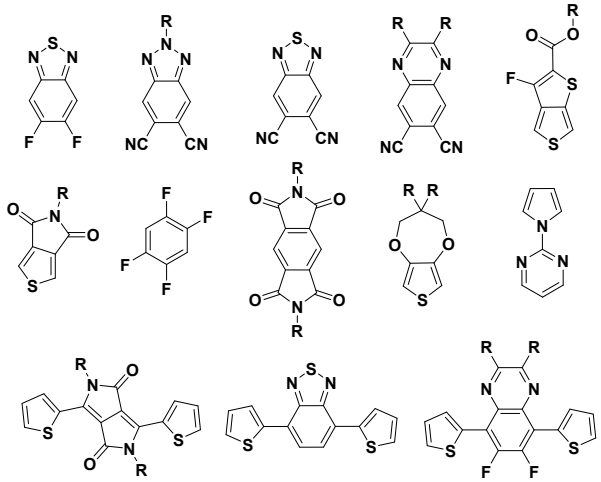

Scheme 14. Typical C-H components used in direct arylation polymerization.

The significance of β-defects and branching lies in the potential for cross-linked polymer chains, which can greatly impact packing and result in an insoluble polymer fraction, ultimately reducing the yield of polymerization. Research has shown that even a minor 1.4% branching defect in Poly(3-hexylthiophene (P3HT) can significantly disturb the polymer film morphology and diminish the degree of π-π stacking. [133] This highlights the critical importance of minimizing these defects in order to optimize polymerization efficiency and enhance film quality. Furthermore, it should be noted that the DARP reaction is not a ubiquitous method as it necessitates the presence of reactive C-H bonds in one of the starting monomers, which significantly reduces the range of available starting compounds. Specifically, only unfunctionalized compounds with very strong electron acceptor units can be utilized as the reaction's transition state involves the hydrogen bonding of a Pd-linked carboxylic acid anion with a departing proton. Additionally, electron-withdrawing groups must be present at both reacting positions of the C-H monomer for the reaction to proceed. **Scheme 14** illustrates some commonly used C-H comonomers in DARP, but there are still limitations to overcome, particularly with selectivity as multiple active C-H bonds in the monomer can produce unwanted side reactions and generate various defects. [134-136] For instance, when reacting thiophene rings, a β-defect can arise if the C-H bond in the 3-position reacts instead of the 2-position, leading to branching defects and cross-linking between polymer chains, as well as homo-coupling.

To summarize, various alternative methods have emerged in recent times, each displaying their own set of benefits and limitations. Nevertheless, Stille polycondensation still proves to be a highly effective approach in creating a diverse array of optoelectronic materials.

7. Conclusions and outlook

Stille polycondensation is a versatile synthetic tool that has proved crucial in developing numerous types of semiconductor polymers. This method offers unique advantages over other polymerization techniques, including its broad scope of monomers, tolerance to various functional groups, and mild reaction conditions. Over the past decade, functional materials generated via Stille polycondensation have been instrumental in the advancement of fields such as organic electronics (OPV, OFET, OLED, and OLET) and biological imaging, gas and ion sensing. Despite the remarkable progress made, several challenges remain. For instance, the production of defect-free polymers has been demonstrated to be crucial in achieving consistent and high-quality polymer material performance. While excellent strategies have been documented, it remains a significant challenge to effectively manage and prevent homo-coupling reactions. Thus, addressing this concern is of utmost importance. Additionally, the organotin halide by-products are toxic and must be avoided in the reaction system; furthermore, the use of costly palladium catalysts calls for cost-effective catalytic systems or alternative, versatile methods like direct arylation polymerization or coupling with brominated/iodinated monomers. Nevertheless, the narrow scope of monomers has been a limiting factor for these alternative methods, giving Stille polycondensation an edge. Future research should focus on developing new polycondensation reactions that use nontoxic groups, such as silanes, under efficient catalytic systems and expanding the monomer scope to generate new functions. Stille polycondensation will continue to play a pivotal role in the production of new organic semiconductors, and its utilization will become even more widespread as applications of semiconductor polymers continue to broaden.

AUTHOR INFORMATION

Corresponding Authors

*Xunshan Liu - Key Laboratory of Surface & Interface Science of Polymer Materials of Zhejiang Province，School of Chemistry and Chemical Engineering, Zhejiang Sci-Tech University, 928 Second Street, Hangzhou, 310018, China; orcid.org/0000-0003-1537-258X; Email: xliu350@zstu.edu.cn;

*Luping Yu - Department of Chemistry and The James Franck Institute, The University of Chicago, 929 East 57th Street, Chicago, IL 60637, USA; Email: lupingyu@uchicago.edu.

Author contributions

L. Y. supervised the project, Z. L., A. N., Z. Z., and F. Z. drafted the manuscript, X. L. finalized and revised the manuscript. All the authors discussed and commented on the manuscript.

Notes

There are no conflicts to declare.

ACKNOWLEDGMENT

Financial supports from the National Natural Science Foundation of China (22105172), the Natural Science Foundation of Zhejiang Province (LQ22B040003), the

Fundamental Research Funds of Zhejiang Sci-Tech University (21062113-Y, 23062110-Y), are gratefully acknowledged. This work was made possible via the support of NSF (CHE-2102102).

REFERENCES

1. B. Carsten, F. He, H. J. Son, T. Xu and L. Yu, *Chem. Rev.*, 2011, **111**, 1493-1528.
2. C. Cordovilla, C. Bartolomé, J. M. Martínez-Ilarduya and P. Espinet, *ACS Catal.*, 2015, **5**, 3040-3053.
3. M. García-Melchor, A. A. C. Braga, A. Lledós, G. Ujaque and F. Maseras, *Accounts Chem. Res.*, 2013, **46**, 2626-2634.
4. M. H. Pérez-Temprano, A. M. Gallego, J. A. Casares and P. Espinet, *Organometallics*, 2011, **30**, 611-617.
5. A. L. Casado, P. Espinet, A. M. Gallego and J. M. Martínez-Ilarduya, *Chem. Commun.*, 2001, DOI: 10.1039/B008811K, 339-340.
6. A. L. Casado and P. Espinet, *Organometallics*, 1998, **17**, 954-959.
7. A. Nova, G. Ujaque, F. Maseras, A. Lledós and P. Espinet, *J. Am. Chem.Soc.*, 2006, **128**, 14571-14578.
8. E. D. Sosa Carrizo, I. Fernández and S. E. Martín, *Organometallics*, 2015, **34**, 159-166.
9. L. Lu, T. Zheng, T. Xu, D. Zhao and L. Yu, *Chem. Mater.*, 2015, **27**, 537-543.
10. V. Calò, A. Nacci, A. Monopoli and F. Montingelli, *J. Org. Chem.*, 2005, **70**, 6040-6044.
11. E. O. Pentsak, D. B. Eremin, E. G. Gordeev and V. P. Ananikov, *ACS Catal.*, 2019, **9**, 3070-3081.
12. J. Sherwood, J. H. Clark, I. J. S. Fairlamb and J. M. Slattery, *Green Chem.,* 2019, **21**, 2164-2213.
13. M. n. H. Pérez-Temprano, A. M. Gallego, J. A. Casares and P. Espinet, *Organometallics*, 2011, **30**, 611-617.
14. Y.-J. Cheng, S.-H. Yang and C.-S. Hsu, *Chem. Rev.*, 2009, **109**, 5868-5923.
15. B. Carsten, F. He, H. J. Son, T. Xu and L. Yu, *Chem. Rev.,* 2011, **111**, 1493-1528.
16. J. G. Laquindanum, H. E. Katz, A. J. Lovinger and A. Dodabalapur, *Adv. Mater.,* 1997, **9**, 36-39.
17. W.-H. Chang, L. Meng, L. Dou, J. You, C.-C. Chen, Y. Yang, E. P. Young, G. Li and Y. Yang, *Macromolecules*, 2015, **48**, 562-568.
18. L. Dou, J. Gao, E. Richard, J. You, C.-C. Chen, K. C. Cha, Y. He, G. Li and Y. Yang, *J. Am. Chem. Soc.*, 2012, **134**, 10071-10079.
19. F. He, W. Wang, W. Chen, T. Xu, S. B. Darling, J. Strzalka, Y. Liu and L. Yu, *J. Am. Chem. Soc.*, 2011, **133**, 3284-3287.
20. H. J. Son, L. Lu, W. Chen, T. Xu, T. Zheng, B. Carsten, J. Strzalka, S. B. Darling, L. X. Chen and L. Yu, *Adv. Mater.*, 2013, **25**, 838-843.
21. T. Zheng, L. Lu, N. E. Jackson, S. J. Lou, L. X. Chen and L. Yu, *Macromolecules*, 2014, **47**, 6252-6259.
22. W. Yue, R. S. Ashraf, C. B. Nielsen, E. Collado‐Fregoso, M. R. Niazi, S. A. Yousaf, M. Kirkus, H. Y. Chen, A. Amassian and J. R. Durrant, *Adv. Mater.*, 2015, **27**, 4702-4707.
23. K. J. Fallon, N. Wijeyasinghe, N. Yaacobi-Gross, R. S. Ashraf, D. M. Freeman, R. G.

Palgrave, M. Al-Hashimi, T. J. Marks, I. McCulloch and T. D. Anthopoulos, *Macromolecules*, 2015, **48**, 5148-5154.

24. K. J. Fallon, N. Wijeyasinghe, E. F. Manley, S. D. Dimitrov, S. A. Yousaf, R. S. Ashraf, W. Duffy, A. A. Guilbert, D. M. Freeman and M. Al-Hashimi, *Chem. Mater.*, 2016, **28**, 8366-8378.
25. B. Carsten, J. M. Szarko, H. J. Son, W. Wang, L. Lu, F. He, B. S. Rolczynski, S. J. Lou, L. X. Chen and L. Yu, *J. Am. Chem. Soc.*, 2011, **133**, 20468-20475.
26. A. M. Schneider, L. Lu, E. F. Manley, T. Zheng, V. Sharapov, T. Xu, T. J. Marks, L. X. Chen and L. Yu, *Chem. Sci.*, 2015, **6**, 4860-4866.
27. T. Xu, L. Lu, T. Zheng, J. M. Szarko, A. Schneider, L. X. Chen and L. Yu, *Adv. Funct. Mater.*, 2014, **24**, 3432-3437.
28. L. Dou, W. H. Chang, J. Gao, C. C. Chen, J. You and Y. Yang, *Adv. Mater.*, 2013, **25**, 825-831.
29. R. S. Ashraf, I. Meager, M. Nikolka, M. Kirkus, M. Planells, B. C. Schroeder, S. Holliday, M. Hurhangee, C. B. Nielsen and H. Sirringhaus, *J. Am. Chem. Soc.*, 2015, **137**, 1314-1321.
30. H. Zhong, Z. Li, E. Buchaca-Domingo, S. Rossbauer, S. E. Watkins, N. Stingelin, T. D. Anthopoulos and M. Heeney, *J. Mater. Chem. A*, 2013, **1**, 14973-14981.
31. H. Zhong, Z. Li, F. Deledalle, E. C. Fregoso, M. Shahid, Z. Fei, C. B. Nielsen, N. Yaacobi-Gross, S. Rossbauer and T. D. Anthopoulos, *J. Am. Chem. Soc.*, 2013, **135**, 2040-2043.
32. H. Wang, P. Chao, H. Chen, Z. Mu, W. Chen and F. He, *ACS Energy Lett.*, 2017, **2**, 1971-1977.
33. D. Mo, H. Wang, H. Chen, S. Qu, P. Chao, Z. Yang, L. Tian, Y.-A. Su, Y. Gao, B. Yang, W. Chen and F. He, *Chem. Mater.*, 2017, **29**, 2819-2830.
34. S. Qu, H. Wang, D. Mo, P. Chao, Z. Yang, L. Li, L. Tian, W. Chen and F. He, *Macromolecules*, 2017, **50**, 4962-4971.
35. Z. Hu, H. Chen, J. Qu, X. Zhong, P. Chao, M. Xie, W. Lu, A. Liu, L. Tian, Y.-A. Su, W. Chen and F. He, *ACS Energy Lett.*, 2017, **2**, 753-758.
36. S. Zhang, Y. Qin, J. Zhu and J. Hou, *Adv. Mater.*, 2018, **30**, 1800868.
37. M. Wang, H. Wang, T. Yokoyama, X. Liu, Y. Huang, Y. Zhang, T.-Q. Nguyen, S. Aramaki and G. C. Bazan, *J. Am. Chem.l Soc.*, 2014, **136**, 12576-12579.
38. M. Wang, H. Wang, M. Ford, J. Yuan, C.-K. Mai, S. Fronk and G. C. Bazan, *J. Mater. Chem. A*, 2016, **4**, 15232-15239.
39. I. H. Jung, W.-Y. Lo, J. Jang, W. Chen, D. Zhao, E. S. Landry, L. Lu, D. V. Talapin and L. Yu, *Chem. Mater.*, 2014, **26**, 3450-3459.
40. T. Earmme, Y.-J. Hwang, N. M. Murari, S. Subramaniyan and S. A. Jenekhe, *J. Am. Chem. Soc.*, 2013, **135**, 14960-14963.
41. Y. J. Hwang, B. A. Courtright, A. S. Ferreira, S. H. Tolbert and S. A. Jenekhe, *Adv. Mater.*, 2015, **27**, 4578-4584.

42. Z. G. Zhang, Y. Yang, J. Yao, L. Xue, S. Chen, X. Li, W. Morrison, C. Yang and Y. Li, *Angew. Chem. Int. Ed.*, 2017, **56**, 13503-13507.

43. D. Chen, J. Yao, L. Chen, J. Yin, R. Lv, B. Huang, S. Liu, Z. G. Zhang, C. Yang and Y. Chen, *Angew. Chem. Int. Ed.*, 2018, **57**, 4580-4584.

44. H. Yao, F. Bai, H. Hu, L. Arunagiri, J. Zhang, Y. Chen, H. Yu, S. Chen, T. Liu and J. Y. L. Lai, *ACS Energy Lett.*, 2019, **4**, 417-422.

45. R. Sorrentino, E. Kozma, S. Luzzati and R. Po, *Energ. Environ. Sci.*, 2021, **14**, 180-223.

46. G. Wang, F. S. Melkonyan, A. Facchetti and T. J. Marks, *Angew. Chem. Int. Ed.*, 2019, **58**, 4129-4142.

47. M. Zhang, X. Guo, W. Ma, H. Ade and J. Hou, *Adv. Mater.*, 2015, **27**, 4655-4660.

48. Q. Liu, Y. Jiang, K. Jin, J. Qin, J. Xu, W. Li, J. Xiong, J. Liu, Z. Xiao, K. Sun, S. Yang, X. Zhang and L. Ding, *Sci. Bull. (Beijing)*, 2020, **65**, 272-275.

49. Z. Zheng, H. Yao, L. Ye, Y. Xu, S. Zhang and J. Hou, *Mater. Today*, 2020, **35**, 115-130.

50. Y. Shao, Y. Gao, R. Sun, M. Zhang and J. Min, *Adv. Mater.*, 2023, **35**, e2208750.

51. X. Yuan, Y. Zhao, D. Xie, L. Pan, X. Liu, C. Duan, F. Huang and Y. Cao, *Joule*, 2022, **6**, 647-661.

52. X. Yuan, Y. Zhao, Y. Zhang, D. Xie, W. Deng, J. Li, H. Wu, C. Duan, F. Huang and Y. Cao, *Adv. Funct. Mater.*, 2022, **32**, 2201142.

53. X. Yuan, Y. Zhao, T. Zhan, J. Oh, J. Zhou, J. Li, X. Wang, Z. Wang, S. Pang, P. Cai, C. Yang, Z. He, Z. Xie, C. Duan, F. Huang and Y. Cao, *Energ. Environ. Sci.*, 2021, **14**, 5530-5540.

54. Q. An, J. Wang, W. Gao, X. Ma, Z. Hu, J. Gao, C. Xu, M. Hao, X. Zhang, C. Yang and F. Zhang, *Sci. Bull. (Beijing)*, 2020, **65**, 538-545.

55. Y. Cai, C. Xie, Q. Li, C. Liu, J. Gao, M. H. Jee, J. Qiao, Y. Li, J. Song, X. Hao, H. Y. Woo, Z. Tang, Y. Zhou, C. Zhang, H. Huang and Y. Sun, *Adv. Mater.*, 2023, **35**, e2208165.

56. J. Du, K. Hu, J. Zhang, L. Meng, J. Yue, I. Angunawela, H. Yan, S. Qin, X. Kong, Z. Zhang, B. Guan, H. Ade and Y. Li, *Nat. Commun.*, 2021, **12**, 5264.

57. H. Fu, Y. Li, J. Yu, Z. Wu, Q. Fan, F. Lin, H. Y. Woo, F. Gao, Z. Zhu and A. K. Jen, *J. Am. Chem. Soc.*, 2021, **143**, 2665-2670.

58. Z. Luo, R. Ma, T. Liu, J. Yu, Y. Xiao, R. Sun, G. Xie, J. Yuan, Y. Chen, K. Chen, G. Chai, H. Sun, J. Min, J. Zhang, Y. Zou, C. Yang, X. Lu, F. Gao and H. Yan, *Joule*, 2020, **4**, 1236-1247.

59. F. Peng, K. An, W. Zhong, Z. Li, L. Ying, N. Li, Z. Huang, C. Zhu, B. Fan, F. Huang and Y. Cao, *ACS Energy Lett.s*, 2020, **5**, 3702-3707.

60. R. Sun, W. Wang, H. Yu, Z. Chen, X. Xia, H. Shen, J. Guo, M. Shi, Y. Zheng, Y. Wu, W. Yang, T. Wang, Q. Wu, Y. Yang, X. Lu, J. Xia, C. J. Brabec, H. Yan, Y. Li and J. Min, *Joule*, 2021, **5**, 1548-1565.

61. H. Chen, W. Zhang, M. Li, G. He and X. Guo, *Chem. Rev.*, 2020, **120**, 2879-2949.

62. J. Chen, J. Yang, Y. Guo and Y. Liu, *Adv. Mater.*, 2022, **34**, e2104325.

63. X. Chen, S. Hussain, A. Abbas, Y. Hao, A. H.

Malik, X. Tian, H. Song and R. Gao, *Mikrochim Acta.*, 2022, **189**, 83.

64. M. Kim, S. U. Ryu, S. A. Park, K. Choi, T. Kim, D. Chung and T. Park, *Adv. Funct. Mater.*, 2019, **30**.
65. K. Liu, B. Ouyang, X. Guo, Y. Guo and Y. Liu, *NPJ Flex. Electron*, 2022, **6**.
66. N. Luo, P. Ren, Y. Feng, X. Shao, H. L. Zhang and Z. Liu, *J. Phys. Chem. Lett.*, 2022, **13**, 1131-1146.
67. S. Riera‐Galindo, F. Leonardi, R. Pfattner and M. Mas‐Torrent, *Adv. Mater. Tech.*, 2019, **4**, 1900104.
68. F. Wu, Y. Liu, J. Zhang, S. Duan, D. Ji and H. Yang, *Small Methods*, 2021, **5**, e2100676.
69. Y. Yan, Y. Zhao and Y. Liu, *J. Polym. Sci.*, 2021, **60**, 311-327.
70. Y. Yu, Q. Ma, H. Ling, W. Li, R. Ju, L. Bian, N. Shi, Y. Qian, M. Yi, L. Xie and W. Huang, *Adv. Funct. Mater.*, 2019, **29**.
71. H. Yuan, Z. Li, X. Wang and R. Qi, *Polymers (Basel)*, 2022, **14**, 3657.
72. S. Yuvaraja, A. Nawaz, Q. Liu, D. Dubal, S. G. Surya, K. N. Salama and P. Sonar, *Chem. Soc. Rev.*, 2020, **49**, 3423-3460.
73. J. H. Park, E. H. Jung, J. W. Jung and W. H. Jo, *Adv. Mater.*, 2013, **25**, 2583-2588.
74. I. Kang, T. K. An, J. A. Hong, H. J. Yun, R. Kim, D. S. Chung, C. E. Park, Y. H. Kim and S. K. Kwon, *Adv. Mater.*, 2013, **25**, 524-528.
75. H. J. Yun, S. J. Kang, Y. Xu, S. O. Kim, Y. H. Kim, Y. Y. Noh and S. K. Kwon, *Adv. Mater.*, 2014, **26**, 7300-7307.
76. Z. Zhao, Z. Yin, H. Chen, L. Zheng, C. Zhu, L. Zhang, S. Tan, H. Wang, Y. Guo, Q. Tang and Y. Liu, *Adv. Mater.*, 2017, **29**.
77. C. Zhu, Z. Zhao, H. Chen, L. Zheng, X. Li, J. Chen, Y. Sun, F. Liu, Y. Guo and Y. Liu, *J. Am. Chem. Soc.*, 2017, **139**, 17735-17738.
78. Y. Shi, H. Guo, M. Qin, J. Zhao, Y. Wang, H. Wang, Y. Wang, A. Facchetti, X. Lu and X. Guo, *Adv. Mater.*, 2018, **30**.
79. Y. He, N. A. Kukhta, A. Marks and C. K. Luscombe, *J. Mater. Chem. C.*, 2022, **10**, 2314-2332.
80. H. Lin, H. Bai, Z. Yang, Q. Shen, M. Li, Y. Huang, F. Lv and S. Wang, *Chem. Commun. (Camb)*, 2022, **58**, 7232-7244.
81. S. Sharma, P. Sudhakara, A. A. B. Omran, J. Singh and R. A. Ilyas, *Polymers (Basel)*, 2021, **13**, 2398.
82. H. Sun and K. S. Schanze, *ACS Appl. Mater. Interfaces*, 2022, **14**, 20506-20519.
83. J. Sun, Q. Zhang, X. Dai, P. Ling and F. Gao, *Chem. Commun. (Camb)*, 2021, **57**, 1989-2004.
84. Y. Wang, L. Feng and S. Wang, *Adv. Funct. Mater.*, 2019, **29**.
85. Y. Wu, C. Shi, G. Wang, H. Sun and S. Yin, *J. Mater. Chem. B*, 2022, **10**, 2995-3015.
86. L. Xiao, X. Chen, X. Yang, J. Sun and J. Geng, *ACS Appl. Polym. Mater.*, 2020, **2**, 4273-4288.
87. J. Xie, P. Yu, Z. Wang and J. Li, *Biomacromolecules*, 2022, **23**, 641-660.
88. J. Yang, S. Chen, Q. Liu, Y. Wang, Z. Miao, X. Ren, Y. Hu, G. Zhang, H. Dong, Y. Qiao, Y. Song and W. Hu, *Sci. China Mater.*, 2023, **66**, 2436–2444.

89. L. Zhou, F. Lv, L. Liu and S. Wang, *Acc. Chem. Res.*, 2019, **52**, 3211-3222.
90. L. Li, R. G. Hadt, S. Yao, W.-Y. Lo, Z. Cai, Q. Wu, B. Pandit, L. X. Chen and L. Yu, *Chem. Mater.*, 2016, **28**, 5394-5399.
91. D. Giri and S. K. Patra, *RSC Adv.*, 2015, **5**, 79011-79021.
92. Y. Cao, J.-H. Dou, N.-j. Zhao, S. Zhang, Y.-Q. Zheng, J.-P. Zhang, J.-Y. Wang, J. Pei and Y. Wang, *Chem. Mater.*, 2016, **29**, 718-725.
93. P. Wang, S. Lin, Z. Lin, M. D. Peeks, T. Van Voorhis and T. M. Swager, *J. Am. Chem. Soc.*, 2018, **140**, 10881-10889.
94. J. Xu, S. Wang, G.-J. N. Wang, C. Zhu, S. Luo, L. Jin, X. Gu, S. Chen, V. R. Feig, J. W. F. To, S. Rondeau-Gagné, J. Park, B. C. Schroeder, C. Lu, J. Y. Oh, Y. Wang, Y.-H. Kim, H. Yan, R. Sinclair, D. Zhou, G. Xue, B. Murmann, C. Linder, W. Cai, J. B. H. Tok, J. W. Chung and Z. Bao, *Science*, 2017, **355**, 59.
95. J. Y. Oh, S. Rondeau-Gagne, Y. C. Chiu, A. Chortos, F. Lissel, G. N. Wang, B. C. Schroeder, T. Kurosawa, J. Lopez, T. Katsumata, J. Xu, C. Zhu, X. Gu, W. G. Bae, Y. Kim, L. Jin, J. W. Chung, J. B. Tok and Z. Bao, *Nature*, 2016, **539**, 411-415.
96. K. Pu, J. Mei, J. V. Jokerst, G. Hong, A. L. Antaris, N. Chattopadhyay, A. J. Shuhendler, T. Kurosawa, Y. Zhou, S. S. Gambhir, Z. Bao and J. Rao, *Adv. Mater.*, 2015, **27**, 5184-5190.
97. K. H. Hendriks, W. Li, G. H. Heintges, G. W. van Pruissen, M. M. Wienk and R. A. Janssen, *J. Am. Chem. Soc.*, 2014, **136**, 11128-11133.
98. G. Pirotte, J. Kesters, T. Cardeynaels, P. Verstappen, J. D'Haen, L. Lutsen, B. Champagne, D. Vanderzande and W. Maes, *Macromol. Rapid. Commun.*, 2018, **39**, e1800086.
99. M. Spanos, V. G. Gregoriou, A. Avgeropoulos and C. L. Chochos, *Macromol. Chem. Phys.*, 2017, **218**, e1700283.
100. W. T. Neo, Q. Ye, Z. Shi, S.-J. Chua and J. Xu, *Mater. Chem. Front.*, 2018, **2**, 331-337.
101. M. R. Raj, M. Kim, H. I. Kim, G.-Y. Lee, C. W. Park and T. Park, *J. Mater. Chem. A*, 2017, **5**, 3330-3335.
102. S. Kim, J. K. Park and Y. D. Park, *RSC Adv.*, 2014, **4**, 39268-39272.
103. Q. Wang, B. Zhang, L. Liu, Y. Chen, Y. Qu, X. Zhang, J. Yang, Z. Xie, Y. Geng, L. Wang and F. Wang, *J. Phys. Chem. C*, 2012, **116**, 21727-21733.
104. J. K. Park, J. Jo, J. H. Seo, J. S. Moon, Y. D. Park, K. Lee, A. J. Heeger and G. C. Bazan, *Adv. Mater.*, 2011, **23**, 2430-2435.
105. J. D. Harris and K. R. Carter, *Polym. Chem.*, 2018, **9**, 1132-1138.
106. S. M. Lee, K. H. Park, S. Jung, H. Park and C. Yang, *Nat. Commun.*, 2018, **9**, 1867.
107. B. Ma, Q. Shi, X. Ma, Y. Li, H. Chen, K. Wen, R. Zhao, F. Zhang, Y. Lin, Z. Wang and H. Huang, *Angew. Chem. Int. Ed.*, 2022, **61**, e202115969.
108. Z. Li, Q. Shi, X. Ma, Y. Li, K. Wen, L. Qin, H. Chen, W. Huang, F. Zhang, Y. Lin, T. J. Marks and H. Huang, *Nat. Commun.*, 2022, **13**, 144.

109. V. S. Delgado Filho, P. F. Lopes, P. L. Podratz and J. B. Graceli, *Braz J. Med. Biol. Res.*, 2011, **44**, 958-965.

110. F. Mignini, C. Nasuti, M. Artico, F. Giovannetti, C. Fabrizi, L. Fumagalli, G. Iannetti and E. Pompili, *Int. J. Immunopath. Ph.*, 2012, **25**, 1107-1119.

111. E. Liu, X. Du, R. Ge, T. Liang, Q. Niu and Q. Li, *Food Chem. Toxicol.*, 2013, **60**, 302-308.

112. V. C. Karpiak and C. L. Eyer, *Cell Bio. Toxicol.*, 1999, **15**, 261-268.

113. I. J. Boyer, *Toxicology*, 1989, **55**, 253-298.

114. M. A. Lapitskaya, L. L. Vasiljeva and K. K. Pivnitsky, *Mendeleev Commun.*, 2013, **23**, 257-259.

115. D. P. Curran and C. T. Chang, *J. Org. Chem.*, 1989, **54**, 3140-3157.

116. C. J. Salomon, G. O. Danelon and O. A. Mascaretti, *J. Org. Chem.*, 2000, **65**, 9220-9222.

117. P. Renaud, E. Lacôte and L. Quaranta, *Tetrahedron Lett.*, 1998, **39**, 2123-2126.

118. E. Le Grognec, J. M. Chretien, F. Zammattio and J. P. Quintard, *Chem. Rev.*, 2015, **115**, 10207-10260.

119. S. Xu, E. H. Kim, A. Wei and E. I. Negishi, *Sci Technol Adv. Mater.*, 2014, **15**, 044201.

120. J. R. Pouliot, F. Grenier, J. T. Blaskovits, S. Beaupre and M. Leclerc, *Chem. Rev.*, 2016, **116**, 14225-14274.

121. J. T. Blaskovits and M. Leclerc, *Macromol. Rapid. Commun.*, 2019, **40**, e1800512.

122. P. S. Hegger, J. Kupka, B. B. Minsky, S. Laschat and H. Boehm, *Molecules*, 2018, **23**.

123. K. Nakabayashi, *Polym. J.*, 2018, **50**, 475-483.

124. R. Matsidik, H. Komber, M. Brinkmann, K. S. Schellhammer, F. Ortmann and M. Sommer, *J. Am. Chem. Soc.*, 2023, **145**, 8430-8444

125. F. Livi, N. S. Gobalasingham, B. C. Thompson and E. Bundgaard, *J. Polym. Sci. Part A: Polym. Chem.*, 2016, **54**, 2907-2918.

126. A. V. Akkuratov, F. A. Prudnov, A. V. Chernyak, P. M. Kuznetsov, A. S. Peregudov and P. A. Troshin, *J. Polym. Sci. Part A: Polym. Chem.*, 2019, **57**, 776-782.

127. A. Robitaille, S. A. Jenekhe and M. Leclerc, *Chem. Mater.*, 2018, **30**, 5353-5361.

128. P. Berrouard, A. Najari, A. Pron, D. Gendron, P. O. Morin, J. R. Pouliot, J. Veilleux and M. Leclerc, *Angew. Chem. Int. Ed.*, 2012, **51**, 2068-2071.

129. D. Zimmermann, C. Sprau, J. Schröder, V. G. Gregoriou, A. Avgeropoulos, C. L. Chochos, A. Colsmann, S. Janietz and H. Krüger, *J. Polym. Sci. Part A: Polym. Chem.*, 2018, **56**, 1457-1467.

130. G. Marzano, D. Kotowski, F. Babudri, R. Musio, A. Pellegrino, S. Luzzati, R. Po and G. M. Farinola, *Macromolecules*, 2015, **48**, 7039-7048.

131. R. Matsidik, H. Komber, A. Luzio, M. Caironi and M. Sommer, *J. Am. Chem. Soc.*, 2015, **137**, 6705-6711.

132. A. S. Dudnik, T. J. Aldrich, N. D. Eastham, R. P. Chang, A. Facchetti and T. J. Marks, *J. Am. Chem. Soc.*, 2016, **138**, 15699-15709.

133. K. Okamoto, J. B. Housekeeper, F. E. Michael and C. K. Luscombe, *Polym. Chem.* 2013, **4**, 3499-3506.

134. A. E. Rudenko and B. C. Thompson, *J. Polym. Sci. Part A: Polym. Chem.*, 2015, **53**, 135-147.

135. T. J. Aldrich, A. S. Dudnik, N. D. Eastham, E. F. Manley, L. X. Chen, R. P. H. Chang, F. S. Melkonyan, A. Facchetti and T. J. Marks, *Macromolecules*, 2018, **51**, 9140-9155.

136. F. Lombeck, H. Komber, S. I. Gorelsky and M. Sommer, *ACS Macro. Lett.*, 2014, **3**, 819-823.